Published in final edited form as:
Circ Cardiovasc Imaging. 2016 October ; 9(10): . doi:10.1161/CIRCIMAGING.116.005131.

Optimization and Reproducibility of Aortic Valve 18F-Fluoride Positron Emission Tomography in Patients with Aortic Stenosis

Tania A Pawade, MD[1], **Timothy RG Cartlidge, MD**[1], **William SA Jenkins, MD**[1], **Philip D Adamson, MD**[1], **Phillip Robson, PhD**[2], **Christophe Lucatelli, PhD**[3], **Edwin JR Van Beek, MD, PhD**[3], **Bernard Prendergast, DM FRCP FESC**[4], **Alan R Denison, MD**[5], **Laura Forsyth, BSc, PhD**[6], **James HF Rudd, PhD, FRCP, FESC**[7], **Zahi A Fayad, PhD**[2], **Alison Fletcher, PhD**[3], **Sharon Tuck, BSc, MSc**[8], **David E Newby, MD**[1], and **Marc R Dweck, MD, PhD**[1]

[1]BHF/Centre for Cardiovascular Science, University of Edinburgh, UK

[2]Translational and Molecular Imaging Institute, Icahn School of Medicine at Mount Sinai, New York

[3]Clinical Research Imaging Centre, Queen's Medical Research Institute, University of Edinburgh

[4]Guys and St Thomas' Hospitals NHS Foundation Trust

[5]Institute for Education in Medical and Dental Sciences. University of Aberdeen

[6]Edinburgh Clinical Trials Unit, Western General Hospital, University of Edinburgh, UK

[7]Division of Cardiovascular Medicine, University of Cambridge

[8]Wellcome Trust Clinical Research Facility, Western General Hospital Edinburgh

Abstract

Background—18F-Fluoride positron emission tomography (PET) and computed tomography (CT) can measure disease activity and progression in aortic stenosis. Our objectives were to optimize the methodology, analysis and scan-rescan reproducibility of aortic valve 18F-fluoride PET-CT imaging.

Methods and Results—Fifteen patients with aortic stenosis underwent repeated 18F-fluoride PET-CT. We compared non-gated PET and non-contrast CT, with a modified approach that incorporated contrast CT and ECG-gated PET. We explored a range of image analysis techniques including estimation of blood-pool activity at differing vascular sites and a most-diseased segment (MDS) approach. Contrast-enhanced ECG-gated PET-CT permitted localization of 18F-fluoride uptake to individual valve leaflets. Uptake was most commonly observed at sites of maximal mechanical stress: the leaflet tips and the commissures. Scan-rescan reproducibility was markedly improved using enhanced analysis techniques leading to a reduction in percentage error from ±63% to ±10% (tissue-to-background ratio MDS mean of 1.55, bias -0.05, limits of agreement -0·20 to +0·11).

Correspondence to Tania Pawade, MD, Chancellor's Building, University of Edinburgh, 49 Little France Crescent, EH16 4SB, Tania.pawade@ed.ac.uk.

Disclosures
None.

Europe PMC Funders Author Manuscripts

Conclusions—Optimized 18F-fluoride PET-CT allows reproducible localization of calcification activity to different regions of the aortic valve leaflet and commonly to areas of increased mechanical stress. This technique holds major promise in improving our understanding of the pathophysiology of aortic stenosis and as a biomarker end-point in clinical trials of novel therapies.

Clinical Trial Registration—URL: http://www.clinicaltrials.gov. Unique identifier: NCT02132026.

Keywords

positron emission tomography; aortic valve stenosis; 18F-fluoride; calcification; valvular heart disease

Europe PMC Funders Author Manuscripts

Aortic stenosis is the most common form of valve disease in the western world and a major health care burden that is set to treble by 2050. However we currently lack any disease-modifying therapies. Calcification appears to be the predominant pathological process driving disease progression leading to major interest in novel treatment strategies aimed at reducing calcification activity in the valve 1. However assessing the efficacy of new therapies requires large trials with prolonged follow-up to demonstrate an impact on disease progression and clinical end-points 2. A non-invasive imaging technique capable of measuring calcification activity in the valve would be highly desirable to assess treatment efficacy in phase 2 clinical trials.

18F-Fluoride is a positron-emitting radiotracer that binds to regions of newly developing microcalcification beyond the resolution of computed tomography 3. It is readily taken up by the valves of patients with aortic stenosis and on histology, correlates with markers of calcification activity 4. Importantly this technique predicts disease progression both with respect to echocardiography and CT calcium scoring as well as adverse cardiovascular events 5–7. 18F-Fluoride positron emission tomography (PET) imaging therefore holds major promise as a marker of calcification activity in aortic stenosis and is an exploratory secondary end-point in the on-going SALTIRE2 clinical trial (NCT02132026). Briefly, this is a randomized controlled trial investigating the ability of therapies targeting calcium metabolism (denosumab and alendronic acid) to modify disease progression in aortic stenosis.

Here, we sought to optimize 18F-fluoride PET scanning of the aortic valve, reduce the effects of cardiac motion and assess the scan-rescan reproducibility of this technique to inform its future application as a novel biomarker of calcification activity in clinical trials.

Methods

Study Population

Patients aged over 50 years with mild, moderate and severe calcific aortic stenosis were recruited prospectively from outpatient clinics at the Edinburgh Heart Centre. Aortic stenosis severity was determined by clinical echocardiograms and graded according to according to American Heart Association/ American College of Cardiology guidelines. This is a sub-

study of the ongoing SALTIRE2 clinical trial (NCT02132026), consequently patients had to meet the same exclusion criteria as those entering the main trial. These included renal failure and women of childbearing potential (full list in supplementary data, Table 1). The study was approved by the Scottish Research Ethics Committee and has a Clinical Trial Authorization from the Medicines and Healthcare products Regulatory Authority (MHRA) of the United Kingdom. It was performed in accordance with the Declaration of Helsinki. All patients gave written informed consent.

Initial Image Acquisition and Analysis

Each patient underwent 18F-fluoride positron emission tomography (PET) and computed tomography (CT) scanning on two occasions. Patients were given 25 mg of oral metoprolol if their resting heart rate was >65 beats/min before being administered 125 MBq of 18F-fluoride intravenously. After 60 min, patients were imaged with a hybrid PET and CT scanner (Biograph mCT,Siemens). Attenuation-correction CT scans were performed before acquisition of PET data in list mode using a single 30-min bed position centered on the valve in three-dimensional mode. Finally, ECG-gated aortic valve CT calcium scoring and contrast-enhanced CT angiography were performed in diastole and in held expiration.

CT calcium scoring was performed by an experienced operator using dedicated software (Vitrea Advanced, Toshiba systems) on axial views, with care taken to exclude calcium originating from the ascending aorta, left ventricular outflow tract and coronary arteries. The calcium score was recorded in Agatston Units (AU).

Analysis was performed using an OsiriX workstation (OsiriX version 3.5.1 64-bit; OsiriX Imaging Software, Geneva, Switzerland). As previously reported, regions of interest were drawn around the perimeter of the valve on the fused non-gated PET and non-contrast CT images 6. These generated mean and maximum standard uptake values (SUV) for each slice. Averaging these values across the entire valve produced whole valve SUV_{mean} and SUV_{max} values respectively. These SUV values were then corrected for blood pool activity to generate tissue-to-background ratio (TBR): whole-valve $TBR_{mean,}$ and TBR_{max}. The blood pool uptake was determined using SUV_{mean} values averaged from across ROIs drawn on 5 contiguous slices in the brachiocephalic vein. For consistency the most caudal ROI was positioned at the point where the innominate vein joined the brachiocephalic vein 6.

To optimize the spatial localization and scan-rescan reproducibility of 18F-fluoride PET-CT imaging, we assessed different approaches to both image acquisition and image analysis.

Optimisation of PET Image Acquisition

Contrast CT of Aortic Valve—Our original technique required the reorientation and co-registration of non-contrast CT images of the aortic valve. This technique posed several challenges, particularly with respect to aligning with the true plane of the valve and accurately defining its perimeter. Moreover the structure of individual leaflets was not visible on these scans precluding more detailed localization of 18F-fluoride uptake. Contrast CT offered potential solutions to these challenges given its superior anatomical detail and the well-established methodology for finding the true plane of the valve 8 (Figure 1).

ECG-Gated PET Data—PET is susceptible to motion, limiting accurate co-registration and the spatial assessment of PET activity within the valve. As a solution, we employed electrocardiogram (ECG) gating of list mode PET data. These data were reconstructed into 4 gates at 25% intervals of the cardiac cycle. Only data acquired between 50 and 75% of the RR interval were assessed because this period corresponds with diastole when cardiac motion is at a minimum. Given that three quarters of the PET data are therefore discarded, the bedtime was increased to 30 min in order to preserve signal-to-noise.

Optimisation of PET Image Analysis

Measurement Of Blood Pool Activity—The stability of blood pool measurements in the SVC for 18F-fluoride based tracers has recently been questioned 9 and we were concerned about variation in the measured blood-pool activity at different levels of the brachiocephalic vein. We reasoned that this may be explained by the relatively small diameter of this vein rendering it susceptible to partial volume effects, amplified by the very low PET signal in surrounding lung tissue (especially in the cranial aspects of the brachocephalic vein). We hypothesized that sampling blood-pool activity from the center of the right atrium (a much larger structure) may improve the ease and accuracy with which these measurements could be made and the consequent scan-rescan reproducibility. Using the same co-registered PET and CT images of the heart, re-orientated to the plane of the valve, a 2-cm^2 ROI was drawn in the center of the right atrium at the level of the right coronary ostium and again in the same position one slice superiorly. Averaging the mean SUV for these two slices gave an alternative measure of blood-pool activity, which was used to correct valvular uptake measurements using two different approaches. First we used the conventional method of dividing aortic valve SUV measurements by the blood-pool to generate TBR values. Secondly we subtracted the blood-pool value from the valvular uptake, to generate the corrected aortic valve SUV (cSUV) as described recently 9.

Most -diseased Segment and Whole Valve Approach—One of the biggest difficulties in quantifying uptake in the valve is defining its limits in the z-plane. To overcome this challenge, our original whole valve technique was compared to a ‘most-diseased segment’ (MDS) approach where the two contiguous slices with the highest SUV values (frequently in the center of the valve) were averaged to generate $SUV_{MDSmean}$, SUV_{MDSmax} and corresponding TBR values. This is similar to the approach previously used for quantifying 18F-fluorodoexyglucose uptake in carotid and aortic atheroma 10

Scan-Rescan Reproducibility

Scan-rescan repeatability and intra-and inter-observer reproducibility of valvular 18F-fluoride PET quantification was assessed for each of the established and novel image analysis approaches described above. Two experienced operators (TP and TC) quantified uptake values on each of the scan-pairs, on two occasions separated by ≥2-week interval to avoid recall bias. Observers were blinded to both their own previous measurements and those of the other operator.

Spatial Resolution

The effect of our modifications on spatial resolution and scan-rescan reproducibility were then assessed in comparison with the original approach. First we assessed the ability of the technique to localize increased 18F-fluoride activity to individual valve leaflets and their different regions. This was done visually using a standardized method for windowing the fused PET/CT images that incorporated the blood pool activity in RA as the minimum. Scan-rescan and observer agreements were assessed.

Statistical Analysis

Continuous variables were expressed as mean ± standard deviation and categorical variables were expressed as total and percentage. Kappa statistics (with 95% confidence intervals) were used to measure the intra-observer and scan-rescan agreement in presence or absence of 18F-fluoride uptake across coronary cusps. The kappa values were interpreted as follows: poor <0.20, fair 0.21-0.4, moderate 0.41-0.60, good 0.61-0.80 and very good >0.81.

Intra-observer, inter-observer and scan-rescan reproducibility of several 18F-fluoride PET uptake approaches were analyzed and presented using Bland-Altman analysis and percentage error 11. Variability in the different techniques was expressed using the width of the 95% limits of agreement (LOA) from Bland-Altman analyses. For the final approach, we considered the scan re-scan reproducibility to be good and acceptable for use in our future trial if the width of the 95% LOA were within ±0.2 for the $TBR_{MDSmean}$ measurements. Percentage errors for the mean bias were calculated using twice the standard deviation of the difference divided by the overall mean measurements. The intraclass correlation coefficient (ICC) was used to examine the reliability for both intra and inter-observer variability.

Statistical analysis was performed using SAS for Windows version 9.4. Graphs were produced using PRISM version 6.0 for Mac.

Results

Patient Characteristics

Fifteen patients (73±7 years, 67% male) had 2 scans (Table 1), 3.9 ±3.3 weeks apart between November 2014 and May 2015. Seven patients had mild aortic stenosis, 4 had moderate and 4 had severe aortic stenosis. In three participants, the between scan interval exceeded 4 weeks (5 weeks, 8 weeks and 14 weeks). The dose of 18F-fluoride was similar on each visit (123±8 and 125±4 MBq, P=0·49).

Altered PET Acquisition and Image Quality

Good image quality allowing complete image analysis was achieved on all 15 scan-pairs. The prolonged bed-times of 30 min did not result in increased patient motion during the 18F-Fluoride PET scans. The impact of each stepwise change in the acquisition and analysis protocol on scan-rescan reproducibility is summarized in Table 2.

On visual assessment contrast CT imaging of the valve provided much clearer anatomical detail of the leaflets and valve structure compared to non-contrast CT (Figure 2). This made

it technically easier to get into the true plane of the valve and allowed more accurate regions of interest to be drawn around its perimeter (Figure 1 and 2). Co-registration with ECG-gated PET data then allowed localization of 18F-fluoride uptake to individual leaflets and their different regions. This was previously impossible using non-contrast CT and non-gated PET. Most commonly increased activity was observed across all three coronary cusps (n=10), it involved two cusps in 4 patients, and was isolated to one cusp in just 1 patient. The non-coronary cusp was involved in all patients apart from that latter case. Activity was most frequently observed at the valve commissures: the point where the valve cusps meet the aortic ring [n=10] and at the tips where the leaflets coapt during diastole (n=8) (Figure 2).

When examining intra-observer reproducibility for detecting the presence or absence of 18F-fluoride uptake on individual valve leaflets, this was ‘very good’ for the right coronary cusp (kappa=1.00), ‘good’ for the non coronary cusp (kappa=0.63) and ‘moderate’ for the left (kappa=0.58) coronary cusps. The scan-rescan agreement was ‘good’ for the right (kappa=0.76), ‘good’ for the non (kappa=0.63) and ‘very good’ for the left (kappa=0.81) coronary cusps (Tables 3 and 4).

Effect of Altered Image Analysis on PET Reproducibility

Interobserver and intra-observer reproducibility was good using both the original and modified approaches as previously reported. ICC values for intra and inter-observer reproducibility were 0.88 and 0.80 respectively (Table 5). However the scan-rescan reproducibility of our original approach produced percentage errors of ±26% and ±27% for the mean and maximum SUV measurements respectively (Table 2). Scan re-scan reproducibility for TBR measurements were disappointing with percentage errors of ±63% and ±65%.

Blood pool measurements—The percentage error of our original TBR values was double that of the SUV values suggesting a problem with our blood-pool measurements. Interestingly a step-wise and non-physiological reduction in our original brachio-cephalic vein measurements was observed on moving cranially up the axial slices away from the heart and into the lung. On average a 20% difference in values was observed between the top and bottom slices but this difference could be as high as 66%. By comparison, blood-pool sampling from the right atrium was easier to perform, allowed larger regions of interest to be drawn and was consistent, demonstrating a <1% difference in measurements acquired on adjacent slices (Figure 3).

Sampling the blood pool in the right atrium led to a substantial improvement in the scan-rescan reproducibility of all our TBR measurements. Indeed after implementing this approach, the reproducibility of our TBR values consistently outperformed those for SUV values with percentage errors of between ±12% and ±22% for mean and maximum values respectively. In contrast, the approach of subtracting the blood pool uptake from the tissue SUV to produce cSUV measures did not greatly improve reproducibility resulting in percentage errors of ±43% and ±39% for mean and maximum measurements respectively despite similar limits of agreement (Table 2).

Considerable variation was observed in 18F-fluoride blood pool PET activity across our population (blood pool SUV 1.10±0.35) and even between different scans on the same patients. This is likely related to physiological variation in the distribution of the tracer.

MDS Approach—The MDS technique improved the technical ease of image analysis, removing the difficulty in deciding upon the upper and lower limits of the valve in the z-plane. This translated into further improvements in scan-rescan reproducibility for mean TBR values with the percentage error for $TBR_{MDSmean}$ measurements reduced to ±10%. Similarly maximum TBR values were optimized upon addition of the MDS approach (percentage error TBR_{MDSmax} ±14%) as were the SUV measurements (percentage errors: $SUV_{MDSmean}$ ±25%, SUV_{MDSmax} ±25%; Table 2).

Final Approach: Addition of Contrast-CT and ECG-gated PET—The addition of contrast CT and ECG-gated PET data, whilst markedly improving image quality as described above, did not have a major effect on scan-rescan reproducibility. Reproducibility of our final approach however, remained good with a percentage error of ±10% for $TBR_{MDSmean}$ measurements (Figure 4). This, combined with its ability to localise PET uptake to individual leaflets, made the final approach our preferred strategy. $TBR_{MDSmean}$ values using the final approach did not show any proportional bias with disease severity (Supplemental data Figure 1) and were again superior to the equivalent $SUV_{MDSmean}$ values (percentage error ±35%) and to measurements quantifying maximum valvular 18F-fluoride uptake, which were less reproducible after the addition of gated-PET and contrast-CT (percentage errors: SUV_{MDSmax} ±50% and TBR_{MDSmax} ±37% respectively) (Table 2).

Discussion

In this study we have systematically investigated the acquisition and analysis of 18F-fluoride PET imaging of the aortic valve. First we have improved the spatial localization of tracer uptake using ECG-gated PET data and contrast CT imaging, so that activity can now be localized to individual leaflets and regions within those leaflets. This has demonstrated that calcification activity is most commonly observed at sites of maximal mechanical stress: in particular in regions of leaflet coaptation and at the commissures. Second we have improved the scan-rescan reproducibility by using blood pool sampling of right atrium and the MDS methodology, and ultimately demonstrated good agreement for repeat $TBR_{MDSmean}$ measurements in the valve (percentage error ±10%). This has important implications for application to future clinical trials, indicating that 18F-fluoride might provide a useful imaging end-point of drug efficacy.

In this study we have modified our previous image acquisition protocol to include contrast-enhanced CT imaging of the aortic valve, thereby providing greater definition of the individual valve leaflets and their components. Moreover we have included ECG-gated PET data to reduce the effects of cardiac motion and more accurately localize the pattern of activity on to the valve. The combined effect of these changes has been to improve the spatial localization of PET activity within the valve, which after accurate 3D co-registration, is now possible within specific regions of individual leaflets. This has demonstrated that 18F-fluoride activity predominantly localizes to sites of increased mechanical stress within

the valve, supporting mechanical injury as a key driver to the disease process. For example 18F-fluoride activity was observed at the edges of the valve leaflets exactly at the sites of leaflet impact during valve closure. Additionally uptake was observed at the valve commissures where mechanical stress is concentrated before being transferred to the aortic wall 12, 13. Whilst these findings need to be confirmed in larger studies with further refinement of thresholding techniques, they here provide key insight into the triggers to calcification activity in aortic stenosis and the importance of mechanical injury. Recent data have indicated that the relationship between the valve calcium burden and hemodynamic obstruction is not perfect 14, 15. The ability of PET to accurately localize calcification activity may be useful in trying to understand whether calcium formation at different sites of the valve has different hemodynamic impacts.

We have modified our image analysis protocol, optimizing the scan-rescan reproducibility of 18F-fluoride imaging in the aortic valve using several different approaches. To date, it has been standard practice for 18F-fluorodeoxyglucose PET to measure the blood pool SUV in the brachiocephalic vein 16. This has the benefit of avoiding contamination of myocardial 18F-fluorodeoxyglucose uptake that would overestimate the blood pool activity if measured in the heart. However, this benefit does not exist for 18F-fluoride, which has no background myocardial uptake. We therefore measured blood pool activity in both the right atrium and the brachiocephalic vein. Measurements in the right atrium are easily performed on the en face (short-axis) images of the valve and resulted in much more consistent blood-pool measurements. Moreover this approach led to a dramatic improvement in the scan-rescan reproducibility of our TBR measurements such that they then outperformed equivalent SUV measures. We believe that sampling the blood-pool activity in the right atrium improved reproducibility because these measurements are less susceptible to the partial volume effects of adjacent lung tissue and because any minor inaccuracies in co-registration with the PET signal will not have a great impact. Furthermore it appears important to correct for variations in background blood pool activity that can occur between scans perhaps due to minor changes in renal function, tracer dose and pharmacokinetic distribution. Chen et al recently surmised that subtracting the blood pool from tissue SUV would improve accuracy 9. However our study findings did not support this and their approach produced lower TBR values thereby increasing the percentage error of our repeat measurements.

Another major improvement in reproducibility was obtained using the most diseased segment (MDS) approach: measuring activity in the two hottest adjacent slices in the valve, rather than attempting to sample the entire valve. The major advantage of this technique is that it removes the considerable difficulty in deciding the limits and boundaries of the valve. Such uncertainty can lead to major differences in valve measurements because uptake is much lower at the extremes of the valve where the volume of tissue is small and inclusion of extraneous tissue will dilute down mean values.

In this manuscript, whilst our stepwise changes to the protocol generally improved the reproducibility of “mean” measures of PET uptake, the effects on “maximum” measures were more variable. This finding is somewhat at odds with experience in oncology where the maximum values are often preferred. This may reflect the use of contrast enhanced CT (not used in cancer imaging), which allowed accurate and reproducible regions of interest to be

drawn around the perimeter of the valve facilitating reproducible measurement of mean PET uptake. In addition it may reflect ECG-gating of the PET data, which discards 75% of the counts, potentially having a greater detrimental impact on maximum values (which rely on counts from only a few pixels and are therefore particularly susceptible to noise) than mean values. It is possible that advanced image analysis approaches that model and correct for cardiac motion without discarding any PET data will improve the reproducibility of TBR_{MDSmax} measurements as has recently been described for coronary 18F-fluoride activity 17.

This is the first study to assess scan-rescan reproducibility for 18F-fluoride uptake in the aortic valve. For a technique to be clinically applicable, clinicians and clinical researchers need the reassurance that a given methodology is robust and reproducible. We have demonstrated this here. However, we acknowledge that scan-rescan reproducibility does not necessary translate to accuracy and sensitivity. The value of 18F-Fluoride as an imaging marker of calcification activity will ultimately be determined by its ability to predict disease progression and to detect changes in calcification activity in response to novel therapies. These aspects are both currently being studied within the SALTIRE 2 clinical trial. We have already shown that the $TBR_{MDSmean}$ can predict disease progression and clinical events in patients with aortic stenosis 18. We can now report $TBR_{MDSmean}$ measurements, made using our optimized image acquisition and analysis protocols, quantify valvular 18F-fluoride activity with good reproducibility and a 10% error. This translates directly into the requirement for low patient numbers for studies investigating the effects of interventions on 18F-fluoride PET uptake (as a marker of calcification activity), because any true effect will not be swamped by 'noise' within the measuring technique. Indeed based upon our reproducibility data, we have provided estimates of the sample sizes required for different effect sizes (Figure 4). For example, 57 patients would be required in each group to detect a 10% difference in mean 18F-fluoride activity based upon 80% power and an alpha error probability of 0.05. However whilst these estimates provide a framework for minimum sample sizes, they should be interpreted with a degree of caution, because they assume a perfect agreement between changes in the $TBR_{MDSmean}$ signal and underlying changes in valve calcification activity.

Limitations

We acknowledge the small sample size, in this study however it is similar to that used in previous studies examining the reproducibility of vascular PET 19and in part reflects attempts to minimize the radiation exposure associated with repeat PET/CT imaging. Moreover whilst previous studies have indicated that 18F-fluoride uptake correlates with histological markers of calcification activity and accurately predicts the progression in the CT calcium score, we currently lack data to show that 18F-fluoride is modifiable with drug therapy. Largely this is because no drug has yet demonstrated an ability to reduce disease activity in aortic stenosis and we lack reliable animal models of this condition.

In conclusion, we have optimized 18F-fluoride PET-CT imaging in the aortic valve. Excellent localization of the PET signal within the aortic valve is now possible, with uptake observed in regions of maximal mechanical stress. Moreover quantification of valvular 18F-

fluoride uptake is now possible with good scan-rescan reproducibility. 18F-Fluoride PET-CT holds major promise as a method to better understand calcification activity in aortic stenosis and as a surrogate endpoint in clinical trials assessing the efficacy of potential therapeutic interventions.

Supplementary Material

Refer to Web version on PubMed Central for supplementary material.

Acknowledgements

We acknowledge the support of staff at the Edinburgh Heart Centre at the Royal Infirmary of Edinburgh, the radiography and radiochemistry staff of the Clinical Research Imaging Centre. We also acknowledge the Edinburgh Clinical Trials Unit and the Trial Steering Committee for the SALTIRE 2 clinical trial.

Sources of Funding

The study was funded by the British Heart Foundation (FS/14/78/31020). TAP, TRGC, and WSAJ, MRD and DEN are supported by the British Heart Foundation (SS/CH/09/002/26360, FS/13/77/30488, SS/CH/09/002/2636, FS/14/78/31020, CH/09/002). DEN is the recipient of a Wellcome Trust Senior Investigator Award (WT103782AIA). MRD is the recipient of the Sir Jules Thorn Award for Biomedical Research 2015. PA is supported by New Zealand Overseas Training and Research Fellowship (1607) and Edinburgh and Lothians Health Foundation (50-534). The Wellcome Trust Clinical Research Facility and the Clinical Research Imaging Centre are supported by NHS Research Scotland (NRS) through NHS Lothian. JHFR is part-supported by the NIHR Cambridge Biomedical Research Centre, the British Heart Foundation and the Wellcome Trust.

References

1. Pawade TA, Newby DE, Dweck MR. Calcification in Aortic Stenosis: The Skeleton Key. J Am Coll of Cardiol. 2015; 66:561–77. [PubMed: 26227196]
2. Rossebo AB, Pedersen TR, Boman K, Brudi P, Chambers JB, Egstrup K, Gerdts E, Gohlke-Barwolf C, Holme I, Kesaniemi YA, Malbecq W, et al. Intensive lipid lowering with simvastatin and ezetimibe in aortic stenosis. N Eng J Med. 2008; 359:1343–56.
3. Irkle A, Vesey AT, Lewis DY, Skepper JN, Bird JL, Dweck MR, Joshi FR, Gallagher FA, Warburton EA, Bennett MR, Brindle KM, et al. Identifying active vascular microcalcification by (18)F-sodium fluoride positron emission tomography. Nat Commun. 2015; 6:7495. [PubMed: 26151378]
4. Dweck MR, Jenkins WS, Vesey AT, Pringle MA, Chin CW, Malley TS, Cowie WJ, Tsampasian V, Richardson H, Fletcher A, Wallace WA, et al. 18F-sodium fluoride uptake is a marker of active calcification and disease progression in patients with aortic stenosis. Circulation Cardiovasc Imaging. 2014; 7:371–8.
5. Dweck MR, Jenkins WS, Vesey AT, Pringle MA, Chin CW, Malley TS, Cowie WJ, Tsampasian V, Richardson H, Fletcher A, Wallace WA, et al. 18F-NaF Uptake Is a Marker of Active Calcification and Disease Progression in Patients with Aortic Stenosis. Circulation Cardiovasc Imaging. 2014; 7:371–8.
6. Dweck MR, Jones C, Joshi NV, Fletcher AM, Richardson H, White A, Marsden M, Pessotto R, Clark JC, Wallace WA, Salter DM, et al. Assessment of valvular calcification and inflammation by positron emission tomography in patients with aortic stenosis. Circulation. 2012; 125:76–86. [PubMed: 22090163]
7. Jenkins WSA, S A, Pringle MAH, Cowie WJA, Richardson H, Fletcher A, Pessotto R, Boon NA, Rudd JHF, Newby DE, Dweck MR. 18F-NaF is a predictor of progression and outcome in Aortic Valve Disease. J Am Coll Cardiol 2014. 2014; 63(12_S) 101016/S0735-1097(14)60995-5.
8. Litmanovich DE, Ghersin E, Burke DA, Popma J, Shahrzad M, Bankier AA. Imaging in Transcatheter Aortic Valve Replacement (TAVR): role of the radiologist. Insights Imaging. 2014; 5:123–45. [PubMed: 24443171]

9. Chen W, Dilsizian V. PET assessment of vascular inflammation and atherosclerotic plaques: SUV or TBR? J Nucl Med. 2015; 56:503–4. [PubMed: 25722451]
10. Fayad ZA, Mani V, Woodward M, Kallend D, Abt M, Burgess T, Fuster V, Ballantyne CM, Stein EA, Tardif JC, Rudd JH, et al. Safety and efficacy of dalcetrapib on atherosclerotic disease using novel non-invasive multimodality imaging (dal-PLAQUE): a randomised clinical trial. Lancet. 2011; 378:1547–59. [PubMed: 21908036]
11. Critchley LA, Critchley JA. A meta-analysis of studies using bias and precision statistics to compare cardiac output measurement techniques. J Clin Monit Comput. 1999; 15:85–91. [PubMed: 12578081]
12. Aikawa E, Nahrendorf M, Sosnovik D, Lok VM, Jaffer FA, Aikawa M, Weissleder R. Multimodality molecular imaging identifies proteolytic and osteogenic activities in early aortic valve disease. Circulation. 2007; 115:377–86. [PubMed: 17224478]
13. Deck JD, Thubrikar MJ, Schneider PJ, Nolan SP. Structure, stress, and tissue repair in aortic valve leaflets. Cardiovasc Res. 1988; 22:7–16. [PubMed: 3167931]
14. Clavel MA, Messika-Zeitoun D, Pibarot P, Aggarwal SR, Malouf J, Araoz PA, Michelena HI, Cueff C, Larose E, Capoulade R, Vahanian A, et al. The complex nature of discordant severe calcified aortic valve disease grading: new insights from combined Doppler echocardiographic and computed tomographic study. J Am Coll of Cardiol. 2013; 62:2329–38. [PubMed: 24076528]
15. Dweck MR, Chin C, Newby DE. Small valve area with low-gradient aortic stenosis: beware the hard hearted. J Am Coll of Cardiol. 2013; 62:2339–40. [PubMed: 24076527]
16. Tawakol A, Migrino RQ, Bashian GG, Bedri S, Vermylen D, Cury RC, Yates D, LaMuraglia GM, Furie K, Houser S, Gewirtz H, et al. In vivo 18F-fluorodeoxyglucose positron emission tomography imaging provides a noninvasive measure of carotid plaque inflammation in patients. J Am Coll of Cardiol. 2006; 48:1818–24. [PubMed: 17084256]
17. Rubeaux M, Joshi N, Dweck MR, Fletcher A, Motwani M, Thomson LE, Germano G, Dey D, Li D, Berman DS, Newby DE, et al. Motion correction of 18F-sodium fluoride PET for imaging coronary atherosclerotic plaques. J Nucl Med. 2015; 57:54–9. [PubMed: 26471691]
18. Jenkins WS, Vesey AT, Shah AS, Pawade TA, Chin CW, White AC, Fletcher A, Cartlidge TR, Mitchell AJ, Pringle MA, Brown OS, et al. Valvular (18)F-Fluoride and (18)F-Fluorodeoxyglucose Uptake Predict Disease Progression and Clinical Outcome in Patients With Aortic Stenosis. J Am Coll of Cardiol. 2015; 66:1200–1. [PubMed: 26338001]
19. Rudd JH, Myers KS, Bansilal S, Machac J, Rafique A, Farkouh M, Fuster V, Fayad ZA. (18)Fluorodeoxyglucose positron emission tomography imaging of atherosclerotic plaque inflammation is highly reproducible: implications for atherosclerosis therapy trials. J Am Coll of Cardiol. 2007; 50:892–6. [PubMed: 17719477]

Europe PMC Funders Author Manuscripts

Europe PMC Funders Author Manuscripts

Clinical Perspective

18F-Fluoride PET is being increasingly used as a research tool to study calcification activity in the vasculature. It binds preferentially to regions of newly developing microcalcification beyond the resolution of CT and in aortic stenosis correlates closely with calcification activity on histology (alkaline phosphatase staining). Moreover clinical 18F-fluoride PET-CT in aortic stenosis offers accurate prediction of disease progression and adverse cardiovascular events. 18F-Fluoride PET-CT therefore has major potential to improve our understanding of the role of calcification in aortic stenosis and also as a surrogate end-point in studies of novel therapies for this condition. This manuscript adds to current literature demonstrating that optimized 18F-fluoride PET-CT in aortic stenosis can localize calcification activity to individual leaflets and regions of the valve associated with increased mechanical stress. Moreover it shows that the scan rescan reproducibility of aortic valve PET measurements is good, with a percentage error of ±10%. These data strongly support the use of 18F-fluoride PET-CT as a tool to study the mechanisms underlying aortic stenosis and also as an end-point in novel therapies for this common condition.

Europe PMC Funders Author Manuscripts

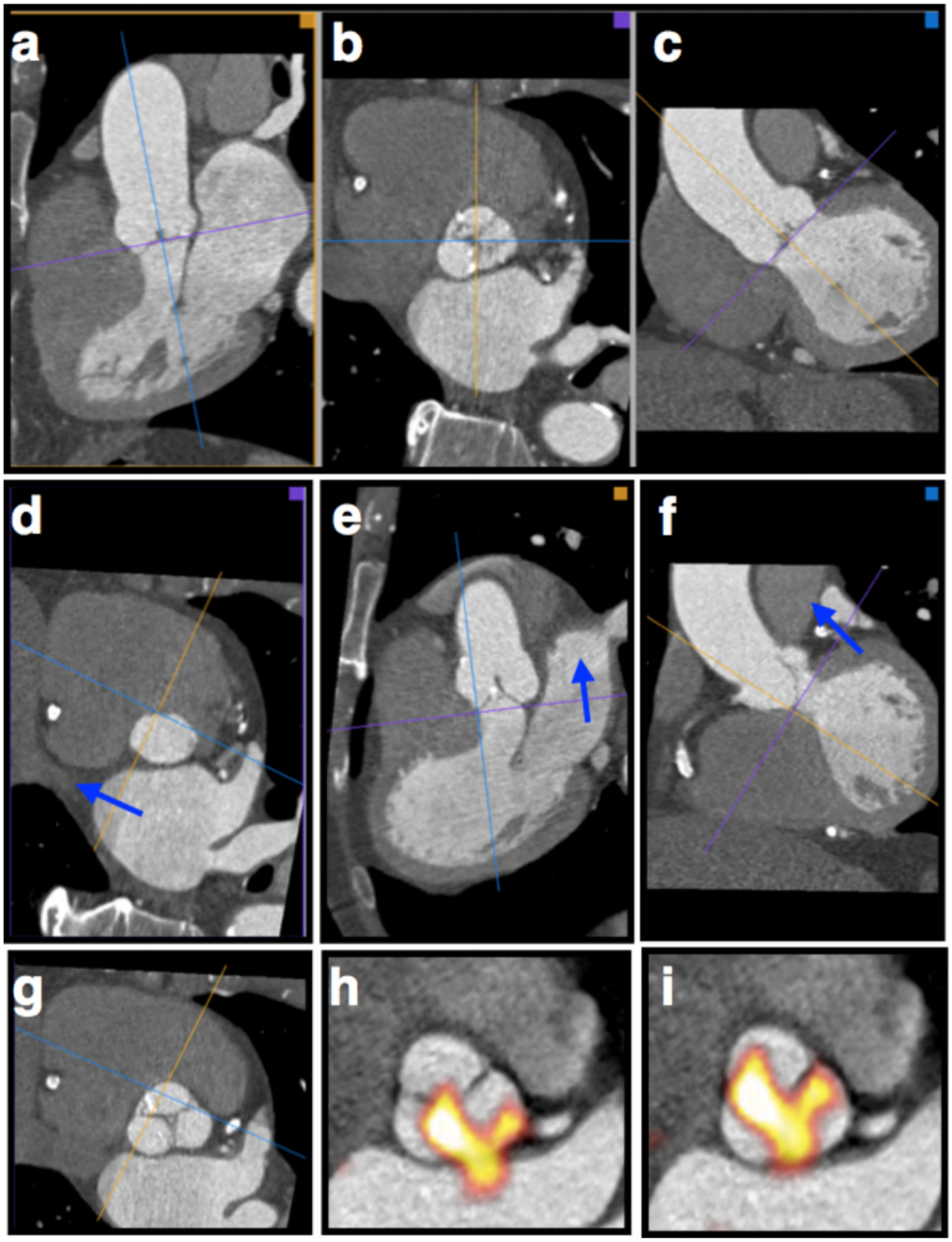

Figure 1. Creation of Co-registered En Face Short-Axis PET/CT Images of the Aortic Valve

Creation of planar en-face valve images using CT angiography was achieved as follows. First, the CT angiogram is reorientated to get into the approximate plane of the aortic valve by lining up the axial cross hair (purple in this example) using the images in the coronal (a) and sagittal planes (c). This creates an approximate cross sectional image of the aortic valve in the axial frame (b). Scrolling down in the axial frame, the center of the crosshairs is then placed over the exact point at which the right coronary cusp disappears, identifying the base of that leaflet (d). Similarly the base of the non-coronary cusp is identified and orthogonal

planes adjusted so that the purple plane goes through the base of both these two cusps (d). Finally the base of the left coronary cusp is found by rotation of the axial cross hairs so that first the cusp comes into view. The image is then slowly rotated in the opposite direction until the point where the leaflet first disappears (the base) is again found (f). This produces an en face image of the valve aligned with the base of all three leaflets (g). Adjacent 3-mm slices are then created in that plane and used for subsequent assessment. These slices are fused with the 18F-Fluoride PET images (h) and careful co-registration performed in 3-dimensions to ensure accurate alignment between the PET and CT images (i).

Europe PMC Funders Author Manuscripts

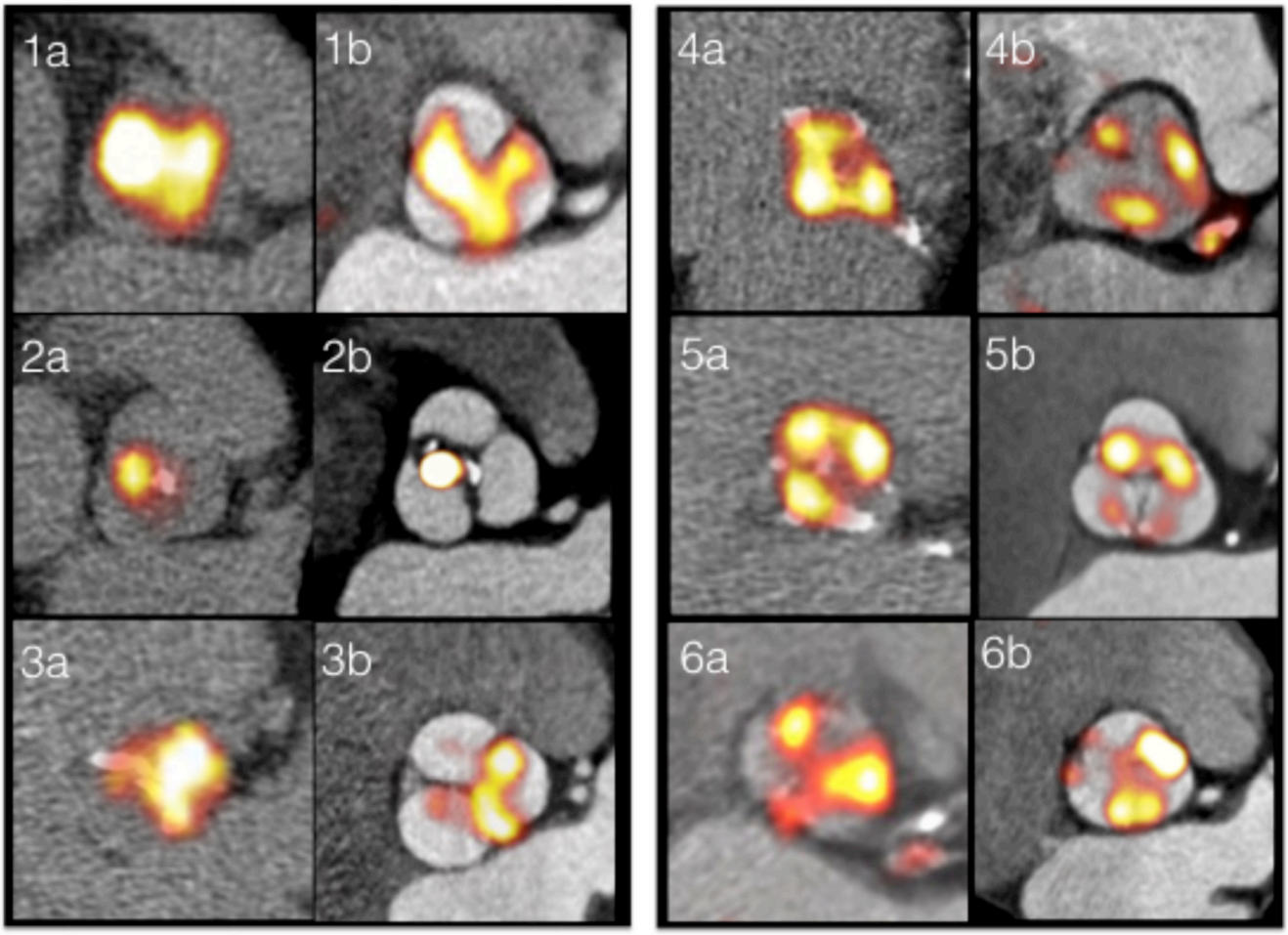

Figure 2. Improved Localization of PET Signal Within the Aortic Valve and its Leaflets

Paired non-gated, non-contrast PET/CT scans (Original approach 1a-6a) and gated, contrast-enhanced PET/CT images (Final approach 1b-6b). Images demonstrate the typical distribution of the tracer uptake within the valve at sites of increased mechanical stress i.e. at the leaflet tips (left: 1,2 and 3) and at the commissures (right: 4,5,6).

Europe PMC Funders Author Manuscripts

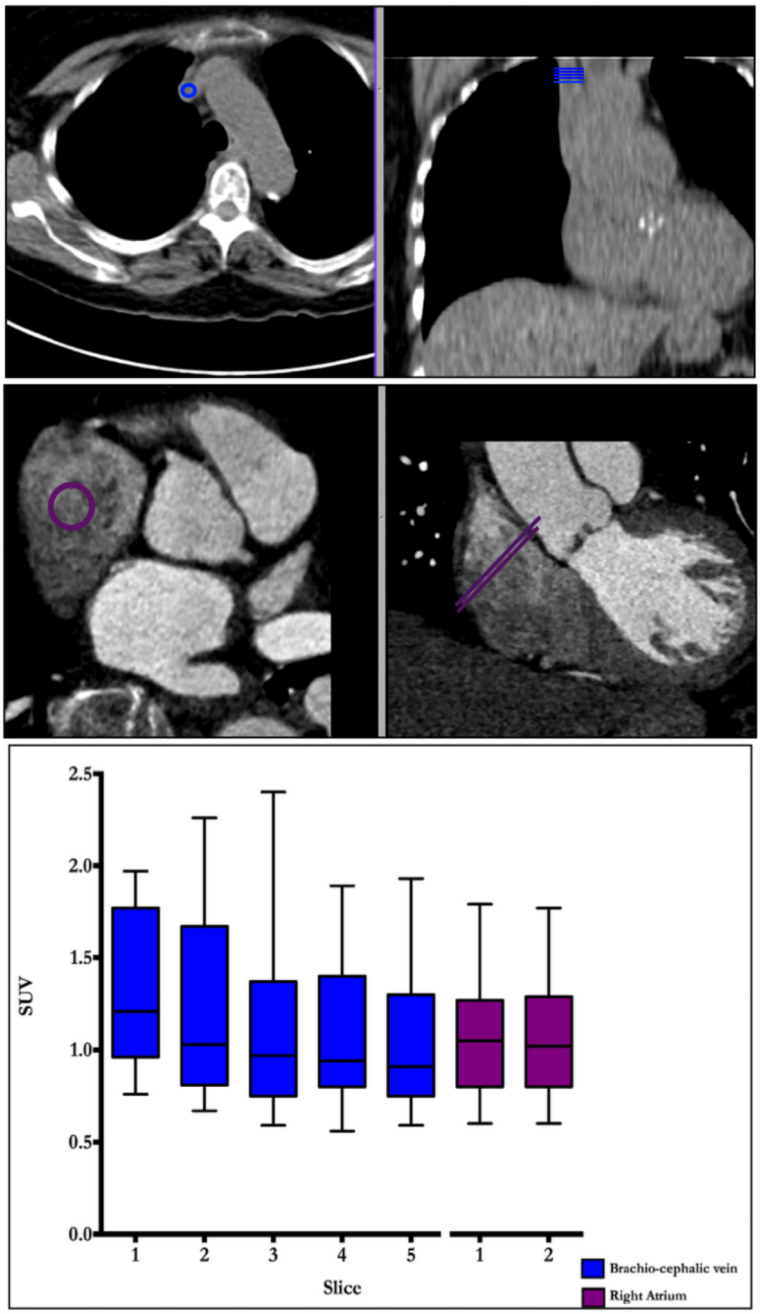

Figure 3. Measuring Blood Pool Activity in the Brachiocephalic vein and the Right Atrium

Regions of interest for measuring blood pool activity in the brachiocephalic vein (top) and right atrium (bottom) are shown in the en-face of the valve (left) and coronal (right) planes. Note that the right atrium is a much larger structure allowing for larger regions of interest with less potential for partial volume artifact problems related to poor registration. Tukey plot demonstrates mean SUV values for 5 contiguous slices from brachiocephalic (blue) and 2 from the right atrium (purple). Note the variation in brachocephalic vein measurements between those taken most caudally versus those taken most cranially.

Europe PMC Funders Author Manuscripts

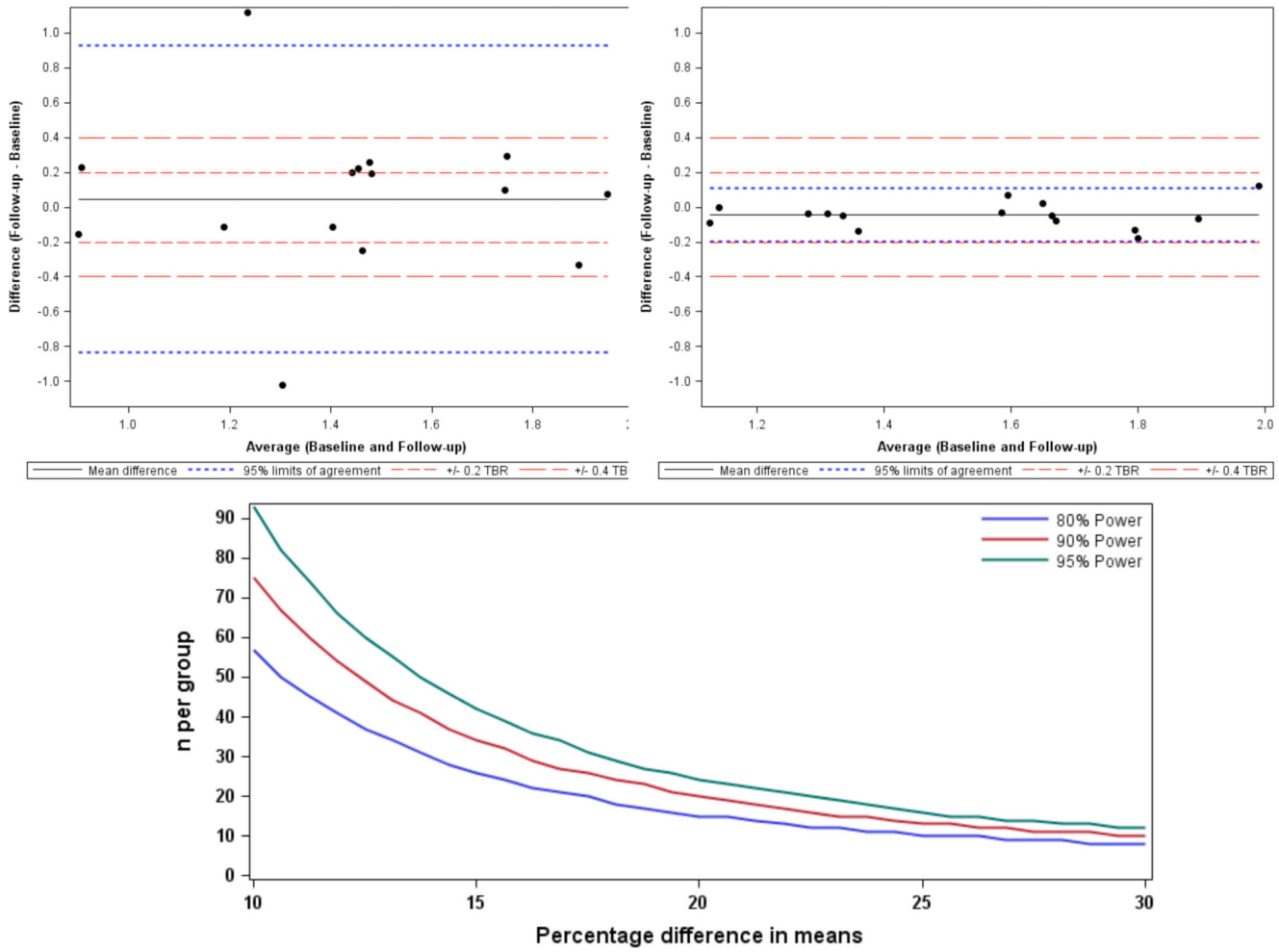

Figure 4. Scan-rescan Reproducibility for 18F-Fluoride PET quantification in the aortic valve with consequent sample size estimates

Bland Altman plots of scan-rescan reproducibility for $TBR_{MDSmean}$ measurements using the original image analysis and acquisition methods (left) and then using final method (right). Percentage error for the final method is less than ±10%. Graph (below) shows the sample size estimates needed to detect differences in means which range from 10%to 30% of the initial scan point estimate. The plot illustrates the sample size required to detect differences in means ranging from 10% to 30% with figures shown for 80, 90 and 95% power. In all cases this assumes that the common standard deviation is 18.75%.

Europe PMC Funders Author Manuscripts

Table 1

Patient Characteristics

		N (%) Total =15
Demographics		
Age (years)		73.3 ± 7.4
Male		10 (67)
Vital Signs		
Body Mass Index (kg/m^2)*		29.7 ± 5.6
Pulse (beats/min)*		67.7 ± 15.5
Body Surface Area (m^2)*		1.9 ± 0.2
Mean Arterial Pressure (mmHg)*		100.1 ± 9.3
Smoker Status	*Current*	1 (7)
	Never	9 (60)
	Ex	5 (33)
Symptoms		
Chest Pain		4 (27)
Breathlessness		7 (47)
Syncope		2 (13)
Duration between scans		
Weeks*		3.9 ± 3.3
Relevant medical history		
Hypertension		11 (73)
Previous CABG		2 (13)
Previous PCI		4 (27)
Liver Disease		1 (7)
Rheumatic Fever		0 (0)
Previous MI		3 (20)
Hypercholesterolemia		10 (67)
Diabetes		4 (27)
Renal Disease		0 (0)
TIA/CVA		2 (13)
Laboratory Results		
Serum Creatinine (mg/dL)*		70.1 ± 11.2
Normal eGFR		14 (93)
Concomitant medications		
ACE inhibitor		6 (40)
AIIRB		3 (20)
Beta Blocker		7 (47)
Statin		9 (60)

Europe PMC Funders Author Manuscripts

Table 2

Bland-Altman values and percentage errors for each stepwise change to the image acquisition and analysis technique.

	MEAN VALUES					MAXIMUM VALUES				
	Overall mean	Difference		95% limits of agreement	% error	Overall mean	Difference		95% limits of agreement	% error
		Mean	Std. Dev				Mean	Std. Dev		
ORIGINAL APPROACH										
Whole Valve, ungated PET, non-contrast CT										
ORIGINAL Standard Uptake Value	1.523	0.008	0.194	-0.373 to 0.389	26	1.955	0.094	0.263	-0.421 to 0.608	27
ORIGINAL Tissue to Background Ratio (using brachiocephalic)	1.439	0.047	0.451	-0.836 to 0.930	63	1.869	0.154	0.612	-1.045 to 1.354	65
RA blood pool correction										
corrected Standard Uptake Value (subtracting RA)	0.425	0.008	0.091	-0.170 to 0.186	43	0.858	0.094	0.168	-0.236 to 0.423	39
Tissue to Background Ratio (using RA)	1.418	-0.002	0.086	-0.171 to 0.167	12	1.842	0.064	0.200	-0.328 to 0.456	22
Most Diseased Segment Approach										
Standard Uptake Value	1.652	0.007	0.207	-0.400 to 0.413	25	2.129	0.131	0.265	-0.389 to 0.651	25
Tissue to Background Ratio (using RA)	1.547	-0.005	0.075	-0.151 to 0.142	10	2.012	0.107	0.145	-0.177 to 0.391	14
FINAL APPROACH										
RA blood pool, most diseased segment, gated PET, contrast CT										
FINAL Standard Uptake Value	1.662	0.044	0.291	-0.527 to 0.615	35	2.528	0.275	0.633	-0.966 to 1.515	50
FINAL Tissue to Background Ratio (using RA)	1.546	-0.046	0.078	-0.199 to 0.107	10	2.385	0.111	0.439	-0.750 to 0.971	37

Table 3

Scan-rescan and intraobserver reproducibility for presence or absence of 18F-fluoride uptake.

	Right coronary Cusp			Non Coronary Cusp			Left Coronary Cusps		
Subject	**1a**	**1b**	**2**	**1a**	**1b**	**2**	**1a**	**1b**	**2**
1	+	+	+	+	+	+	+	+	-
2	+	+	+	+	+	+	+	+	+
3	+	+	+	-	+	+	-	+	-
4	+	+	+	+	+	+	+	+	+
5	+	+	+	+	+	+	+	+	+
6	+	+	+	-	-	-	-	-	-
7	+	+	+	+	+	+	+	+	+
8	-	-	-	+	+	+	+	+	+
9	+	+	+	+	+	+	+	+	+
10	+	+	+	+	+	+	+	+	+
11	-	-	-	+	+	+	+	+	+
12	+	+	-	+	+	+	-	-	-
13	+	+	+	+	+	+	+	+	+
14	+	+	+	+	+	+	+	-	+
15	+	+	+	+	+	+	+	+	+

Presence or absence of 18F-Fluoride PET signal is denoted (+ and – respectively) for each individual valve leaflet. The distribution of 18-Fluoride signal on scan 1 images (1a) were reassessed (1b) to assess intraobserver reproducibility and compared to scan 2 (2) to determine scan-rescan reproducibility.

Table 4

Kappa Statistics for Interobserver and Scan-rescan agreement for 18F-Fluoride PET signal distribution.

a) Right Coronary Cusp							
		Scan 1 (Reading 2)				**Scan 2**	
		Absence	Presence			Absence	Presence
Scan 1 (1st Reading)	Absence	2	0	**Scan 1 (1st Reading)**	Absence	2	0
	Presence	0	13		Presence	1	12
Intra-observer agreement		1.00, 95% CI (-, -)		**Scan/Rescan agreement**		0.76, 95% CI (0.32, 1.00)	

b) Non Coronary Cusp							
		Scan 1 (Reading 2)				**Scan 2**	
		Absence	Presence			Absence	Presence
Scan 1 (1st Reading)	Absence	1	1	**Scan 1 (1st Reading)**	Absence	1	1
	Presence	0	13		Presence	0	13
Intra-observer agreement		0.63, 95% CI (0.00, 1.00)		**Scan/Rescan agreement**		0.63, 95% CI (0.00, 1.00)	

c) Left Coronary Cusp							
		Scan 1 (Reading 2)				**Scan 2**	
		Absence	Presence			Absence	Presence
Scan 1 (1st Reading)	Absence	2	1	**Scan 1 (1st Reading)**	Absence	3	0
	Presence	1	11		Presence	1	11
Intra-observer agreement		0.58, 95% CI (0.07, 1.00)		**Scan/Rescan agreement**		0.81, 95% CI (0.47, 1.00)	

The numbers of presence or absence of 18F-Fluoride for right (a), non (b) and left (c) coronary cusps are provided in the tables below. Kappa statistics and 95% confidence intervals for intra-observer [i.e. Scan 1 (1st Reading) vs. Scan 1 (2nd Reading)] and scan/rescan [i.e. Scan 1 (1st Reading) vs. Scan 2] agreement are also shown.

Europe PMC Funders Author Manuscripts

Table 5

Intra/Inter-observer variability of 18F-Fluoride PET Uptake (expressed as a continuous variable)

	Difference		95% limits of agreement	ICC
	Mean	Standard Deviation		
Intra-observer[1]	0.053	0.124	-0.189, 0.296	0.876
Intra-observer[2]	0.028	0.083	-0.134-0.190	0.979
Inter-observer[3]	-0.092	0.166	-0.418, 0.234	0.796

[1] Rater 1 Scan 1 (1st Reading) vs. Rater 1 Scan 1 (2nd Reading)

[2] Rater 2 Scan 1 (1st Reading) vs Rater 2 Scan 1 (2nd Reading)

[3] Rater 1 Scan 1 (1st Reading) vs. Rater 2 Scan 1 (1st Reading)